

## Brownian Diffusion Close to a Polymer Brush

E. Filippidi,<sup>†</sup> V. Michailidou,<sup>‡,§</sup> B. Loppinet,<sup>\*,‡</sup> J. Rühle,<sup>||</sup> and G. Fytas<sup>‡,§</sup>

Department of Biomedical Engineering, Boston University, Boston, Massachusetts 02215, FORTH/Institute of Electronic Structure and Lasers, P.O. Box 1527, 711 10 Heraklion, Greece, Department of Microsystems Engineering, IMTEK, University of Freiburg, George Köhler Allee 103, 79110, Freiburg, Germany, and Department of Materials Science and Technology, University of Crete, Heraklion, Greece

Received December 22, 2006. In Final Form: January 29, 2007

In an effort to control particle diffusion near surfaces, we have studied the dynamics of colloidal hard spheres and soft compliant star copolymers on surfaces coated with polymer brushes using evanescent wave dynamic light scattering. The same experiments provide information on the brush structure and confined particle motion. The penetration into dense polydisperse brushes is size- and solvent-dependent.

### Introduction

With the advance of microfluidics and the miniaturization of processes, a fundamental understanding of how surface properties might affect the overall flow behavior becomes crucial to the design of micrometer-sized devices. For large volume-to-surface ratios, surface effects are not essential, and simple effective boundary conditions can reliably be used. With increasing surface-to-volume ratios, surface effects become dominant and must be taken into account. They can range from no-slip to slip depending on the surface treatment.<sup>1</sup> Colloidal diffusivity close to the surface can offer direct information on the nature of these effects. The case of a hard wall has received significant attention, and the expected hydrodynamic slow-down of particle diffusivity is now well-confirmed experimentally.<sup>2–9</sup> More complex surfaces can lead to a strongly different behavior. A non-wetting, superhydrophobic surface was reported to lead to a small, hardly measurable slow-down of particle diffusivity close to the surface, indicating slip boundary conditions in that case.<sup>9</sup>

Polymer brushes, which are formed when macromolecules are densely attached to solid surfaces, can offer a model of soft penetrable surfaces. They are also known to provide very good lubrication conditions.<sup>10,11</sup> The flow behavior of particles in contact to such penetrable surfaces should depend on both their size and their shape, which are predicted to control the penetration of particles in polymer brushes.<sup>12</sup> The particle–polymer interac-

tions are relevant in nanostructure formation such as in template-driven organization<sup>13</sup> in block copolymer/particle mixtures.<sup>14</sup> It is conceivable that the structure of the chains that ultimately defines the density profile of the brush also controls both how particles penetrate the brush and what their dynamics is. Reciprocally, information on the structure of a brush could be obtained from the particle penetration and diffusion. The latter is useful in view of the lack of scaling arguments on real, polydisperse brushes.<sup>10,11,15–18</sup>

The soft compliant surface should act as a region of increased friction for penetrating particles and as a lubricant for non-penetrating ones, therefore introducing a size-dependent dynamic threshold. We now show how particle penetration<sup>12,14</sup> in the brush can be measured and offer an estimate of the brush height and how different degrees of penetration affect the measured surface diffusivities.

### Experimental Procedures

**Polymer Brush and Particles.** The polystyrene (PS) brush was grown using an azo initiator covalently attached to a glass surface.<sup>19</sup> Molecular weight was controlled by adjusting monomer concentration and polymerization time. The grafting density (0.05 nm<sup>2</sup>) was estimated from the dry film thickness (30 nm) using the number-average molecular weight of the polymer chains. With a molecular weight above 10<sup>6</sup> g/mol and an estimated polydispersity of  $M_w/M_n = 2$ , which leads to a concentration profile broader than the parabolic profile of monodisperse brushes,<sup>20</sup> the PS brush can reach a thickness up to 1  $\mu\text{m}$  in a good solvent such as toluene.<sup>19</sup> Both hard spheres and soft particles were used. The hard spheres are poly(methylmethacrylate) particles with a hydrodynamic radius  $R = 120$  nm (in decalin) and were kindly provided by A. Schoefield, University of Edinburgh. The soft particles are 64-armed star polystyrene–polybutadiene (PS–PB) diblock copolymers with the PS forming an outer shell so that there is no chemical interaction between the stars and the PS brush and were kindly provided by J. Roovers, NRC Ottawa. Their hydrodynamic radius was determined by quasi-elastic light scattering to be  $20 \pm 1$  nm in decalin. All experiments were performed at 25 °C.

<sup>†</sup> Boston University.

<sup>‡</sup> FORTH/Institute of Electronic Structure and Lasers.

<sup>§</sup> University of Crete.

<sup>||</sup> University of Freiburg.

(1) Lauga, E.; Brenner, M. P.; Stone, H. A. The No-Slip Boundary Condition: A Review, *Condens. Matter* **2005**, 501557.

(2) Garnier, N.; Ostrowsky, N. *J. Phys. II* **1991**, 1, 1221.

(3) Lobry, L.; Ostrowsky, N. *Phys. Rev. B* **1996**, 53, 12050.

(4) Hosoda, M.; Sakai, K.; Tagaki, K. *Phys. Rev. E* **1998**, 58, 6275.

(5) Lin, B.; Yu, J.; Rice, S. A. *Phys. Rev. E* **2000**, 62, 3909.

(6) Holmqvist, P.; Dhont, J. K. G.; Lang, P. R. *Phys. Rev. E* **2006**, 74, 21402.

(7) Feitosa, M. I. M.; Mesquita, O. N. *Phys. Rev. A* **1991**, 44, 6677.

(8) Hosoda, M.; Sakai, K.; Takagi, K. *Phys. Rev. E* **1998**, 58, 6275.

(9) Joly, L.; Ybert, C.; Bocquet, L. *Phys. Rev. Lett.* **2006**, 96, 46101.

(10) Milner, S. T. *Macromolecules* **1991**, 24, 3704.

(11) Grest G. *Advances in Polymer Science*; Springer-Verlag: Berlin, 1998; p 38.

(12) (a) Kim, J. U.; Shaugnessy, B. *Phys. Rev. Lett.* **2002**, 89, 238301. (b) *Ibid. Macromolecules* **2006**, 39, 413.

(13) Lee, J.; Thompson, R. B.; Jasnow, D.; Balasz, A. *Phys. Rev. Lett.* **2002**, 89, 55503.

(14) (a) Bockstaller, M.; Lapetnikov, Y.; Margel, S.; Thomas, E. L. *J. Am. Chem. Soc.* **2003**, 125, 5276. (b) Bockstaller, M.; Thomas, E. L. *Phys. Rev. Lett.* **2004**, 93, 166106.

(15) Karim, A.; Satija, S. K.; Douglas, J. F.; Ankner, J. F.; Fetters, L. J. *Phys. Rev. Lett.* **1994**, 73, 3407.

(16) Yakubov, G. E.; Loppinet, B.; Zhang, H.; Rühle, J.; Sigel, R.; Fytas, G. *Phys. Rev. Lett.* **2004**, 92, 115501.

(17) de Gennes, P. G. *Macromolecules* **1980**, 13, 1069.

(18) Binder, K. *Eur. Phys. J. E* **2002**, 9, 293.

(19) Rühle, J.; Prückner, O. *Langmuir* **1998**, 14, 6893.

(20) Cates, M. E.; Milner, S. T.; Witten, T. A. *Macromolecules* **1988**, 21, 2610.

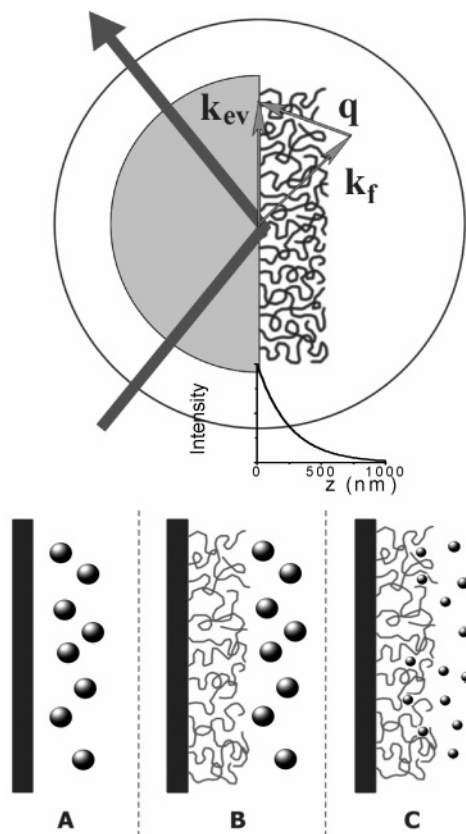


**Figure 1.** Schematic diagram of the evanescent wave dynamic light scattering setup with the laser beam undergoing a total reflection and the evanescent field penetrating within a distance  $\Xi$  from the surface. The wave vectors  $\mathbf{k}_{ev}$  and  $\mathbf{k}_f$  refer to the incident and scattered beams with  $\mathbf{q}$  being the scattering wave vector. Parts A and B illustrate, respectively, the case of the PMMA spheres close to the collapsed PS brush in dodecane and to the soft surface of the swollen PS brush in *cis*-decalin, and part C illustrates PS–PB stars close to the PS brush in *cis*-decalin.

**Light Scattering Technique.** We used evanescent wave dynamic light scattering<sup>21,22</sup> to study the dispersed hard and soft spheres in contact with dense polystyrene brushes. The dynamic structure of the latter in different solvents was recently investigated by this technique.<sup>16,23</sup> The evanescent wave was generated by a total internal reflection of a  $\lambda = 532$  nm laser beam at the flat interface of a semi-cylindrical lens (refractive index  $n = 1.617$ ) to which the brush was end-grafted. The lens–brush system was immersed in the particle solvent solution in the middle of a transparent cylinder, which in turn was placed in a precision  $\theta/2\theta$  goniometer. This allows independent setting of the incident and scattering angles  $\theta_i$  and  $\theta_s$ . The relevant preset experimental parameters are the electric field penetration depth  $\Xi$  [ $1/\Xi = 2\pi n(\sin^2(\theta_i) - \sin^2(\theta_c))^{1/2}/\lambda$ ] and the scattering wave vector  $\mathbf{q} = \mathbf{k}_{ev} - \mathbf{k}_s$ , where  $\theta_c$  is the critical angle and  $\mathbf{k}_s$  and  $\mathbf{k}_{ev}$  are the wave vectors of the scattered and evanescent fields as illustrated in Figure 1. By varying the incidence angle,  $\Xi$  ranges from  $0.2\lambda$  to  $1.5\lambda$ . Because of the presence of strong static surface scattering, the intermediate scattering function  $g(q,t) = \langle I(q,t)I(q,0) \rangle / \langle I(q,0) \rangle^2$  with  $I(q,t)$  being the instantaneous scattering intensity was recorded under heterodyne conditions. The amplitude  $a$  of  $g(q,t)$  at the shortest times ( $\sim \mu s$ ) was low ( $a < 0.05$ ), and the contribution of the physical system (brush/particles) to the total light scattering intensity  $\langle I(q,\Xi) \rangle$  can be estimated by  $I(q,\Xi) = a\langle I(q,\Xi) \rangle$ .  $I(q,\Xi)$  mostly arises from the particles rather than the brush and thus relates

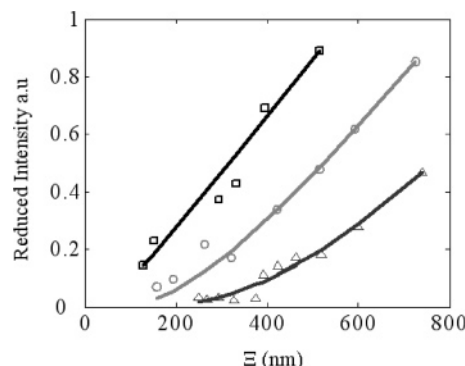


**Figure 2.** Reduced intensity  $I(\Xi)$  profiles for the 120 nm PMMA hard sphere in contact with the collapsed brush in dodecane (squares) and the swollen PS brush in *cis*-decalin (triangles). Circles correspond to the PS–PB stars close to the PS brush in *cis*-decalin (circles). The solid lines indicate the data representation by eq 1 using a step density profile with thicknesses of 30, 160, and 420 nm.

to their thermal density fluctuations (i.e., their self-diffusion). As a consequence of the strong heterodyne conditions, the presented normalized correlation  $C(q,t) = g(q,t)/a$  is expected to be equal to the normalized scattered field autocorrelation function. Because of the exponential decay of the evanescent field with distance  $z$  from the surface (Figure 1),  $g(q,t)$  averages the diffusion behavior of the particles from a volume of characteristic size  $\Xi$  in such a way that the particles closer to the wall are weighted more.

## Results and Discussion

**Particle Penetrability.** We first examine the proximity of the large PMMA spheres to the collapsed brush in dodecane, a non-solvent for PS (but good solvent for the PMMA particles). Measurement of  $I(q,\Xi)$  provides an efficient way to assess the concentration profile,  $c(z)$ , of the particles perpendicular to the wall as

$$I(\Xi) = I(0) \int_z c(z) \exp(-2z/\Xi) dz \quad (1)$$

It was early on recognized<sup>23,24</sup> as a way to estimate the density profile close to a surface (i.e., depletion enrichment; albeit, it was not successfully applied to the best of our knowledge). It should be mentioned that the intensity  $I(\Xi)$  exhibits the  $q$ -dependence anticipated from the form factor of individual PMMA particles excluding any particle aggregation both in the free solution and in the presence of the brush. For the PMMA particles in contact with the collapsed (PS/dodecane) brush,  $I(\Xi)$  was found to be well-fitted, adopting a simple step  $c(z)$  profile as shown in Figure 2a (solid squares). The sample had an excluded layer too small to be accurately measured (30 nm for the line in Figure 2a in agreement with the thickness of the PS layer). In contrast to these test case experiments, a good fit of the experimental  $I(\Xi)$  for the PMMA particles in contact with the swollen brush in decalin (a marginal solvent for PS) (open triangles in Figure 2a) requires us to assume an excluded volume of a height  $L = 430 \pm 30$  nm, clearly demonstrating the exclusion of the particles from the brush. This exclusion of  $2R = 240$  nm PMMA spheres from a dense wet brush that has a very small averaged mesh size  $\xi = \sim 5$  nm<sup>23</sup> is to be expected.<sup>12,13</sup> The excluded thickness value is in agreement with the expected brush thickness (less than  $1 \mu m$ ) and ellipsometry measurements.<sup>15,19</sup>

The level of particle penetration should, however, depend on their size.<sup>12–14</sup> Three regimes might be expected: (i) exclusion for particles with  $R > \xi(z)$ , (ii) complete mixing for particles

(21) Sornette, D.; Lan, K. H.; Ostrowsky, N. *Phys. Rev. Lett.* **1986**, *57*, 17.  
 (22) Fytas, G.; Anastasiadis, S. H.; Seghrouchni, R.; Vlassopoulos, D.; Li, J.; Factor, B. J.; Theobald, W.; Toprakcioglu, C. *Science* **1996**, *274*, 2041.  
 (23) (a) Michailidou, V.; Loppinet, B.; Prücker, O.; Rühle, J.; Fytas, G. *Macromolecules* **2005**, *38*, 8960. (b) *J. Polym. Sci., Part B: Polym. Phys.* **2006**, *44*, 590.

(24) (a) Ausserré, D.; Hervet, H.; Rondelez, F. *Phys. Rev. Lett.* **1985**, *54*, 1948. (b) Polverari, M.; Vandevent, T. G. M. *Langmuir* **1995**, *11*, 1870.

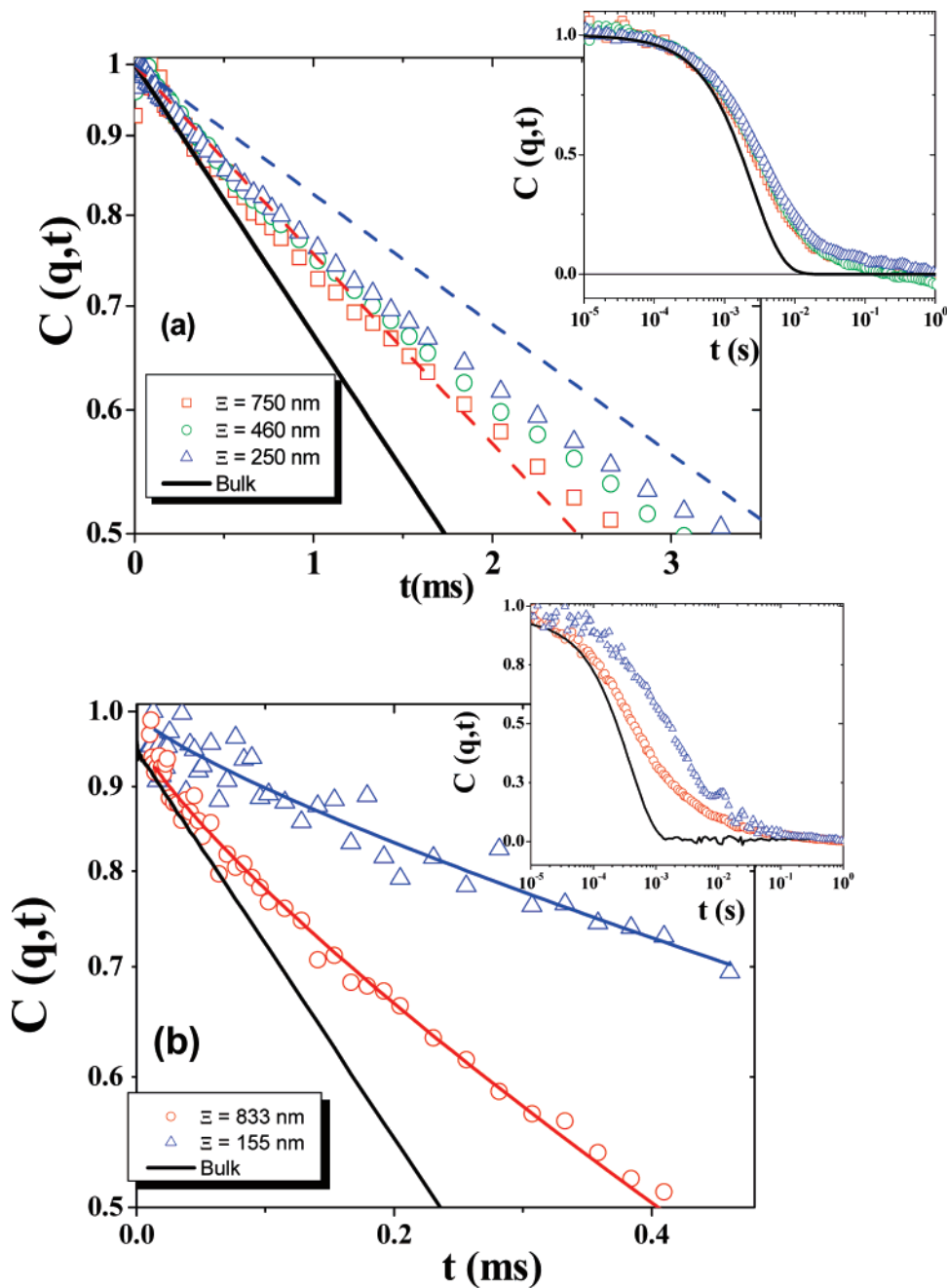


**Figure 3.** Normalized intermediate scattering function  $C(q,t)$  at  $q = 0.025 \text{ nm}^{-1}$  for the particles in contact with the swollen brush in *cis*-decalin at different indicated penetration depths  $\Xi$ . The bulk  $C(q,t)$  is shown in full for comparison. (a) PMMA spheres. A moderate slow-down effect is indicated by the comparison to the free diffusion far from the wall (in the bulk solution) (solid line). Dashed lines represent theoretical early decay of  $C(q,t)$  for diffusion close to the hard wall for penetration depths of 750 and 250 nm. (b) PS–PB stars. Lines are to guide the eye. Both insets present the same correlation functions on a wider time range presented on a logarithmic scale.

with  $2R < \xi(z)$ , and (iii) partial penetration of the upper part of the brush for  $\xi(z)$  and  $2R$  in the same order of magnitude, owing to the  $z$ -dependent brush density profile.<sup>18</sup>

The third case of partial penetration is illustrated by the smaller soft diblock star particles ( $R_h = 20 \text{ nm}$ ), in the same PS brush/decalin system. The fit of  $I(\Xi)$  by a step profile in Figure 2a leads to an excluded layer of size  $160 \pm 20 \text{ nm}$ , much smaller than the 430 nm layer from the PMMA spheres, indicating incomplete penetration of the brush by the particles. We may therefore infer a mesh size of  $\sim 2R_h = 40 \text{ nm}$  at a distance  $z = \sim 160 \text{ nm}$  from the wall, which is otherwise theoretically hard to deduce for a polydisperse brush. Besides this exclusion behavior of the brush and the related structural characterization, the dynamics of the

particles inside the brush up to about 160 nm close to the solid wall can be addressed and is discussed next.

**Particle Diffusion.** We first examine the translational dynamics of the PMMA spheres to validate this expulsive situation since particle mobility is a sensitive index of the environment. Figure 3a displays the normalized  $C(q,t)(=g(q,t)/a)$  relaxation functions at  $\theta = 90^\circ$  for a range of  $\Xi$  values for this system in decalin. The overall shape and dynamics of  $C(q,t)$  (inset of Figure 3a) is nearly insensitive to the variation of  $\Xi$  and slower and broader than the bulk  $C(q,t)$  of the particle diffusion away from the brush (solid line). In evanescent wave dynamic light scattering experiments, quantitative analysis is generally restricted to the short time decay,<sup>2,4,6,21</sup> and the obtained decay rate  $\Gamma$  is related

to a diffusivity averaged over the scattering volume of size  $\Xi$ ,<sup>6</sup>  $\langle D \rangle(\Xi) = \Gamma/(q^2 + \Xi^{-2})$ . With our experimental conditions,  $q\Xi$  remains large ( $q\Xi > 6$ ) and  $\langle D \rangle(\Xi) \sim \Gamma/q^2$  so that the influence of finite penetration depth on the apparent decay rate is negligible. However, deviations from an exponential shape, unexpected for simple diffusion, are observed even at short decay times (Figure 3a) and renders such an analysis difficult.

Despite the non-exponential shape, the good data quality allow some unambiguous conclusions. Figure 3a clearly illustrates the slower decay of the surface correlation (open symbols) as compared to the bulk one (solid line) at the same wave vector  $\mathbf{q}$ . Also shown in Figure 3a are the early exponential decays predicted for diffusion close to a hard wall (broken lines) for two penetration depths. Decay rate values were taken from ref 6, where the averaged diffusivities for  $\Xi = 250$  and  $750$  nm (corresponding to  $\Xi/R = 2.1$  and  $6.2$ ) are found to be  $0.5D_0$  and  $0.7D_0$ , respectively;  $D_0$  denotes the diffusion coefficient in the free bulk solution. Whereas for  $\Xi = 750$  nm, short time particle diffusion is similar near the brush and hard wall, for  $\Xi = 250$  nm, the diffusion dynamics near the brush (open triangles) is visibly faster than near the hard wall (blue dashed line in Figure 3a).

The slow-down of the short time diffusion imposed by the brush on the non-penetrating PMMA particles (as compared to  $D_0$ ) appears to be different than the hydrodynamic slow-down observed near a hard wall. Indeed, the weak  $\Xi$ -dependence observed in the case of the brush implies that the particle diffusivity  $D(z)$  is larger at the brush than at the hard wall. This reduced slow-down of a non-penetrating sphere coming into contact with the permeable wall could originate from the rather large hydrodynamic penetration in a real brush predicted by theory.<sup>10</sup>

Turning to the partially penetrating particles, the low scattered intensity from the smaller particles leads to more noisy correlation

functions (Figure 3b) that nonetheless can provide clear information on the diffusivity of the partially penetrating smaller PS–PB particles. The short time diffusion (symbols) exhibits a strong dependence on the penetration depth, clearly distinct from the previous expelled larger particles (Figure 3a). It was also found to be slower than the unconstrained diffusion far from the brush, in the bulk solution (solid line in Figure 3a). The origin of the observed retarded particle mobility has to be a manifestation of the penetration of the particles within the brush and might be attributed to an increased friction experienced by the smaller PS–PB particles within the brush. As to the microscopic origin of this increased friction, different possibilities arise, but topological confinements trapping the particles in the brush appear to be the most likely. A quantitative evaluation of the slow-down (out of the scope of the present paper) should lead to a determination of trapping time and/or of viscoelastic-like relaxation within the brush in a micro-rheology type of approach [x].

### Conclusion

We have investigated, using evanescent wave dynamic light scattering, the penetration and diffusivities of particles of different sizes in contact with a swollen polymer brush. The penetration depth-dependence of the scattered intensity evidenced a size selective penetration of the particles within the brush. The larger (120 nm) hard spheres were found to be largely expelled from the brush, and their diffusivities were only slightly slowed down, reflecting a certain drag reduction from the brush. The smaller 20 nm softer particles showed a partial penetration of the brush accompanied by slow-down diffusivities. The slower diffusivities of the penetrating particles reflect their increased friction within the brush, providing an indirect structural characterization of the brush.<sup>25</sup>

**Acknowledgment.** E.F. thanks F.O.R.T.H. for their hospitality.

LA0637162

(25) See, for example: Gardel, M. L.; Valentine, M. T.; Weitz, D. A. In *Microscale Diagnostic Techniques*; Breuer, K., Ed.; Springer-Verlag: Berlin, 2005.